Research Journal of Material Sciences _____ ISSN 2320–6055
Vol. **2(5),** 1-10, October **(2014)** *Res. J. Material Sci.*

Inhibiting effect of N,N,N-Trimethyldodecylammonium bromide on Corrosion of mild Steel in 0.5M Sulphuric acid solution, its Adsorption and Kinetic Characteristics

Prathibha B.S.[1], P. Kotteeswaran[2] and V. Bheema Raju[3]
[1]Department of chemistry, BNM Institute of Technology, Bengaluru-70, INDIA
[2]Department of chemistry, RAMCO Institute of Technology, Rajapalayam, Tamil Nadu- 626 117, INDIA
[3]Department of chemistry, Dr. Ambedkar Institute of Technology, Bengaluru, INDIA

Available online at: www.isca.in
Received 27th September 2014, revised 8th October 2014, accepted 15th October 2014

Abstract

The corrosion behavior of mild steel in 0.5M Sulphuric acid containing different concentrations of N,N,N-trimethyldodecylammonium bromide (TDAB) has been studied by weight loss, Tafel polarization and Electrochemical impedance spectroscopic techniques at 298, 308, 318 and 328K respectively. The mild steel samples were also analyzed by scanning electron microscopy. Electrochemical and impedance parameters such as corrosion potential, corrosion current density, Tafel slopes, charge transfer resistance and electrical double layer were determined. The kinetic and thermodynamic parameters for mild steel corrosion and inhibitor adsorption, respectively, were determined and discussed. The results showed that concentration of Inhibitor and test temperatures can affect the % inhibition efficiency. The % corrosion inhibition efficiency increases with increase in concentration and decreases with increase in temperature. The maximum corrosion inhibition efficiency obtained is 95.5%. As the inhibitor concentration increased, the charge transfer resistance increased and double layer capacitance decreased. It was found that TDAB is an excellent inhibitor for mild steel in acidic medium. Adsorption of the inhibitor molecules on the mild steel surface obeyed the Langmuir adsorption isotherm. On the basis of thermodynamic adsorption parameters, comprehensive adsorption for the studied inhibitor on mild steel surface was suggested.

Keywords: Mild steel, corrosion inhibition, Tafel polarization, SEM, Adsorption.

Introduction

The corrosion of mild steel in acidic solutions has been a subject of both academic and industrial concern and has received considerable attention during the last few decades. Among the acids sulphuric acid, is widely used for pickling. However, sulphuric acid is a strong corrosive agent and its corrosivity needs to be controlled. In order to reduce the corrosion of mild steel, several methods have been applied, among them being utilization of organic compounds, and more specifically, cationic surfactants which are gaining high use as corrosion inhibitors. Surfactant have many advantages, for example, high inhibition efficiency, low price, low toxicity and easy production. Surfactants are very beneficial reagents and their presence at very low quantity in any medium provide desirable properties to processes in all industries such as petrochemical, food, paint and coating industry[1]. In the context of corrosion inhibition using surfactants, the critical micelle concentration marks an effective boundary boundary condition below which surfactant adsorption is typically below the monolayer level, and above which adsorption can consists of multiple layers of surfactant. Above the CMC, increasing surfactant concentration leads to the gradual formation of multilayers that can have a similar effect on reducing the rate of corrosion with increasing concentration as concentration changes below the CMC except that the rate of inhibition change is much smaller above the CMC since the surface already contains significant levels of surfactant. Adding surfactant above the CMC is analogous to adding a second coat of paint to protect the surface beyond the protection offered by the initial coat. However, very little work has yet been reported on cationic surfactants as inhibitors for mild steel corrosion in acidic medium.

Atia et al[2] investigated the corrosion inhibition efficiency of Cetylpyridinium chloride on mild steel in 1M H_2SO_4. Dourna Asefi et al [3] studied the corrosion inhibition efficiency of Gemini surfactant 1,4-butan-bis-dimethyl dodecyl ammonium bromide, 1,4-butan-bis-dimethyl tetradecyl ammonium bromide, conventional surfactants dodecyl trimethyl ammonium bromide (DTAB) and tetra decyl trimethyl ammonium bromide(TTAB) on low carbon steel. Fouda et al[4] studied the corrosion inhibition effect of cationic surfactants, namely cetyl trimethyl ammonium bromide (CTAB) and dodecyl trimethyl ammonium chloride (DTAC), on 1037 C-steel in 0.5 M HCl. Abdel Hamid et al[5] investigated the inhibiting effect of cationic surfactant N, N, N-dimethyl 4-methylbenzyl dodecyl ammonium chloride (DMMBDAC) on mild steel in hydrochloric acid solution. Kumar Harish et al[5] studied the corrosion inhibiting behavior of

surfactants, Ammonium decyl sulphate (ADS), ammonium laruryl sulphate (ALS), ammonium hexadecyl sulphate (AHDS) and ammonium dodecyl benzene sulfonate (ADDBS) on carbon steel in 1M HCl solution.

The present study aimed to investigate the efficiency of new surfactant N,N,N-trimethyldodecylammonium bromide(TDAB) as a corrosion inhibitor for mild steel in 0.5M H_2SO_4. An attempt was also made to clarify the effect of concentration and temperature on the inhibition efficiency of studied inhibitor.

Material and Methods

Experimental: The material used in this work was Mild steel with the percentage weight composition, C: 0.223, Mn: 0.505, P: 0.077, Si: 0.164 and Fe: 98.7. For weight loss measurement the specimen were cut into rectangular shape with an exposed area of 2cm x 1cm and were mechanically polished with various grades of emery paper (0/0, 2/0, 4/0 and 6/0) and then cleaned with ethanol and acetone followed by cleaning with double distilled water and finally dried. The working electrode employed for the electrochemical measurements was cylindrical rod of Mild steel welded with copper wire and embedded in Teflon holder using epoxy resin with an exposed area $1cm^2$.

Electrochemical measurements were carried out in a three compartment cell. The counter electrode was platinum foil of $1cm^2$ and the reference electrode was saturated calomel electrode (SCE) with a luggin capillary, which can be at close proximity to the working electrode to minimize ohmic drop.

Measurements were performed in 0.5M H_2S0_4 solution with and without the Inhibitor. The solutions were prepared from bidistilled water. For the weight loss measurement, specimens were weighed by using electronic digital balance (Uni Bloc AUY220 series) and finally suspended in a beaker containing 100ml of acid solution with and without inhibitor. The beakers were kept in a thermostat. After the specified time of immersion (3h), the specimens were removed, washed in distilled water, dried, placed in desiccators to attain room temperature and weighed. The experiments were carried out in triplicate. The corrosion rate was calculated by the relation (1):

$$\text{Corrosion Rate}\left(\frac{\text{mm}}{\text{y}}\right) = \frac{87.6w}{DAT} \quad (1)$$

Where W = weight loss in mg, D = Density (g/cm3), A = area in square centimeter, T= time in hour.

The percentage inhibition efficiency is calculated using the relation (2):

$$\%IE = \frac{W_0 - W_i}{W_0} \quad (2)$$

Where w_i and w_0 are the weight loss values in the presence and in the absence of inhibitor respectively.

The polarization and EIS studies were carried out using CHI Electrochemical workstation model 660C series. The potentiodynamic curves were obtained by scanning the potential range from cathodic potential of -200 mV to an anodic potential of + 200 mV vs SCE with respect to the open circuit potential at a scan rate of 10 mV/S. Equillibrium time leading to the steady state of specimen was 1h and the open circuit potential was noted. The experiments were carried out in triplicate.The percentage corrosion inhibition efficiency was calculated from the relation (3):

$$\%IE = \frac{i^0_{corr} - i_{corr}}{i^0_{corr}} \text{x } 100 \quad (3)$$

Where i^0_{corr} and i_{corr} are the corrosion current densities in absence and presence of various concentrations of the inhibitor.

The electrochemical impedance measurements were performed at corrosion potential over a frequency range 100 KHz to 0.01Hz with signal amplitude of 10 mV. The impedance data were analyzed and fitted using Zsimpwin software. The percentage corrosion inhibition efficiency was calculated using the relation (4):

$$\%IE = \frac{R_{ct} - R^0_{ct}}{R_{ct}} \quad (4)$$

Where R_{ct} and R^0_{ct} are the charge transfer resistance of mild steel with and without inhibitor respectively.

Results and Discussion

Weight loss measurement: The effect of different concentration of inhibitor on the corrosion of mild steel in 0.5M H_2SO_4 solution was studied using the weight loss method at 298K-328K. It can be seen from the table-1 and figure-1 that the inhibition efficiency increases with increase in concentration of TDAB and decreases with increase in temperature.

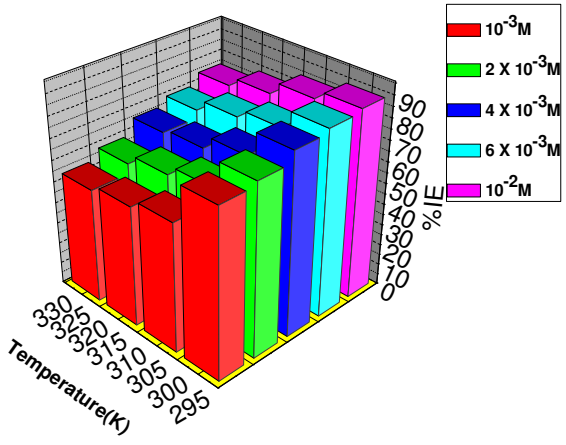

Figure-1
Variation of %IE with temperature and concentration of TDAB

Potentiodynamic Polarization Measurement: The representative potentiodynamic polarization curves for mild Steel in 0.5M H_2SO_4 solution in the absence and presence of various Concentrations of TDAB are shown in the figure-2. From figure-2 it is clearly seen that inhibitor shifted both the anodic and cathodic branches of polarization curves to lower values of current density indicating the inhibition of both hydrogen evolution and mild steel dissolution reactions. Further the shift in the E_{corr} values is < 85mV suggest that the studied inhibitor act as mixed type inhibitor with predominantly of anodic type. The values of corrosion potential (E_{corr}), corrosion current density (i_{corr}), anodic (b_a), cathodic slopes (b_c) and % inhibition efficiency (%IE) in the presence of TDAB for mild steel in 0.5M H_2SO_4 are given in Table-2.

Table-1
Inhibition efficiency of various concentrations of the inhibitor for the corrosion of mild steel in 0.5M H_2SO_4 by weight loss method at different temperatures (298K-328K)

Temperature									
Inhibitor	Inhibitor concentration (M)	298		308		318		328	
		%IE	Corrosion rate(mm/y)	%IE	Corrosion rate(mm/y)	%IE	Corrosion rate(mm/y)	%IE	Corrosion rate(mm/y)
TDAB	Blank	-	59.88	-	112.89	-	225.8	-	410.1
	$1 X 10^{-3}$	78.6	12.83	60.4	44.64	56.6	98.01	53.8	189.5
	$2 X 10^{-3}$	80.4	11.72	67.8	36.27	63.2	83.14	58.4	170.5
	$4 X 10^{-3}$	85.4	8.74	73.8	29.57	67.7	72.91	65.7	140.6
	$6 X 10^{-3}$	87.3	7.62	78.7	23.99	74.8	56.91	69.4	125.5
	$1 X 10^{-2}$	88.8	6.69	84.8	17.11	78.8	47.79	74.6	104.1

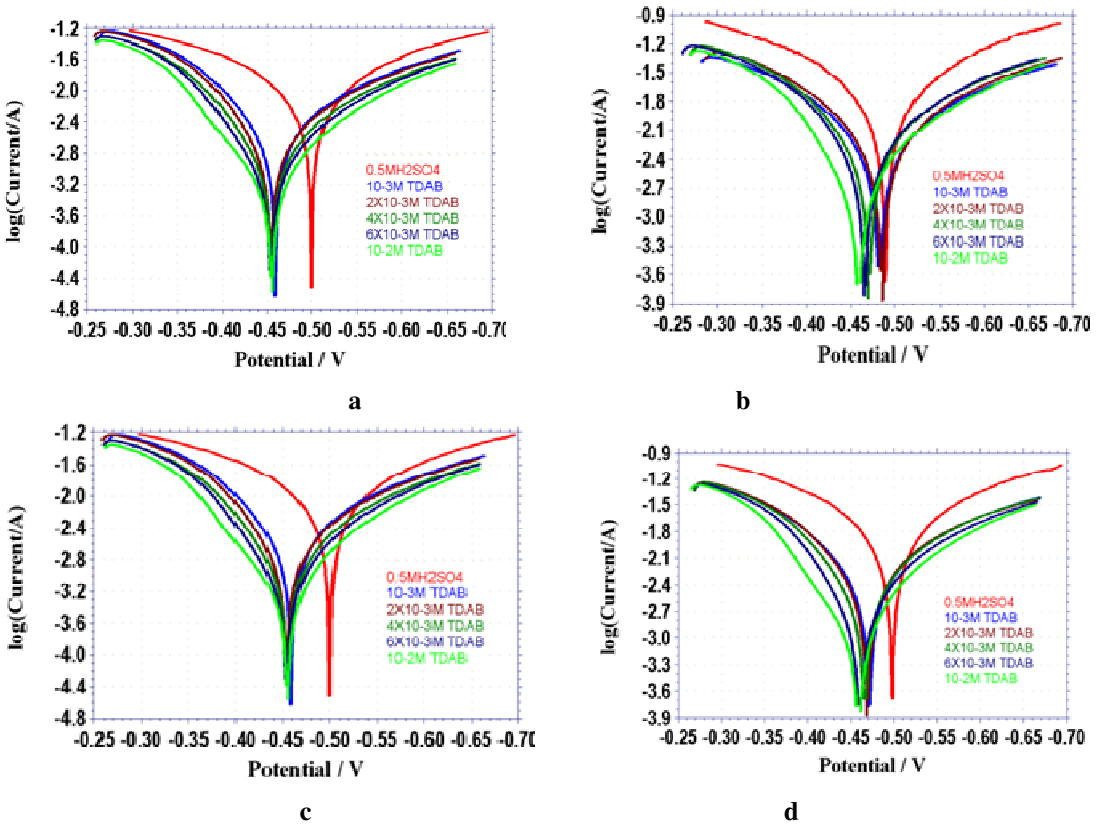

Figure-2
Tafel plots for mild steel in 0.5M H_2SO_4 in the absence and presence of different concentrations of TDAB at a) 298 K b)308K c) 318K and d) 328K

Table-2
Electrochemical polarization parameters for Mild Steel in 0.5M H_2SO_4 containing different concentration of TDAB at different temperatures

Concentration (M)	E_{corr} (mV)	I_{corr} (μA/cm^2)	b_c (mV/decade)	b_a (mV/decade)	% IE
Blank	-502.8	5997	162.6	159.5	-
1 X 10^{-3}	-465.1	977.9	123.4	95.7	83.7
2 X 10^{-3}	-462.8	909.3	119.1	94.3	84.8
4X 10^{-3}	-468.5	581.4	111.5	82.0	90.3
6 X 10^{-3}	-472.3	390.0	107.2	72.1	93.5
1 X 10^{-2}	-466.3	268.3	100.6	61.7	95.5
308 K					
Blank	-497.1	10530	186.9	189.4	-
1 X 10^{-3}	-465.0	3411	173.9	118.2	67.6
2 X 10^{-3}	-458.9	2608	163.2	113.9	75.2
4 X 10^{-3}	-459.8	1713	152.2	101.9	83.7
6 X 10^{-3}	-460.4	1154	139.1	88.2	89.0
1 X 10^{-2}	-460.5	717.8	129.6	71.7	93.2
318 K					
Blank	-495.4	18910	201.9	203.9	-
1 X 10^{-3}	-470.5	6273	187.3	148.7	66.8
2 X 10^{-3}	-467.7	6077	192.8	143.9	67.8
4 X 10^{-3}	-469.1	4436	176.1	127.9	79.6
6 X 10^{-3}	-466.6	2742	160.9	114.2	85.5
1 X 10^{-2}	-465.3	1429	143.6	81.0	92.4
328 K					
Blank	-485.9	27230	201.1	196.2	-
1 X 10^{-3}	-483.1	9980	200.5	170.2	63.3
2 X 10^{-3}	-487.8	9305	196.6	158.4	65.8
4 X 10^{-3}	-470.1	6893	188.1	148.6	74.7
6 X 10^{-3}	-460.6	6301	177.0	152.4	76.7
1 X 10^{-2}	-476.0	2716	160.3	116.6	89.3

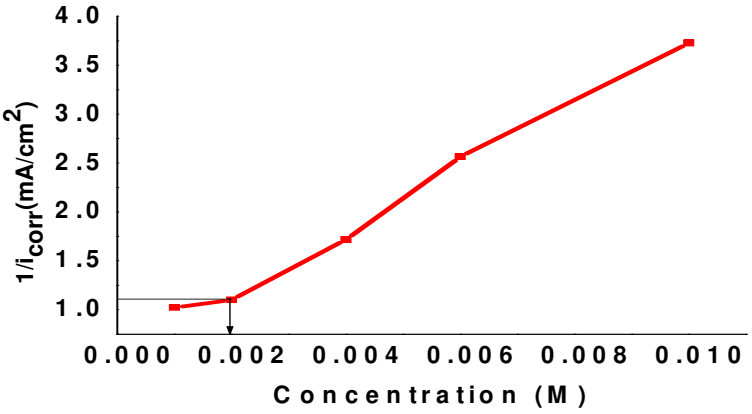

Figure-3
The relation between $1/i_{corr}$ and concentration of the TDAB in 0.5M H_2SO_4 solution

The values of corrosion current decreased significantly with increase in the concentration of TDAB. Corrosion potential values shifted towards more noble direction with increase in the concentration of TDAB. The percentage inhibition efficiency increased with increase in the concentration of inhibitor. The inhibition effect of the surfactants mainly depends upon the critical micelle concentration (CMC). CMC is a key factor in determining the effectiveness of surfactants as corrosion inhibitors. According to Free [6], CMC can be determined by plotting $1/i_{corr}$ against surfactant concentration. From the figure-3 the value of CMC for TDAB is found to be approximately 2×10^{-3}M.

From the Figure-3 it is evident that above the CMC, increasing surfactant concentration leads to the gradual formation of multilayers that further reduces the rate of corrosion thereby increasing the percentage corrosion inhibition efficiency. However, concentration changes above CMC lead to smaller changes in inhibition, since the changes above the CMC result only in additional coverage beyond the monolayer level, which is already sufficient for significant inhibition. This situation is analogous to adding a second coating of paint to protect a surface that is already protected by an initial coating. It is likely that additional surface coverage in the form of multilayer that results at surfactant concentrations above the CMC are responsible for the additional increase in corrosion inhibition above the CMC. The reason for this explanation is simple. At coverages of one monolayer or less, surfactant molecules can inhibit either the cathodic or anodic reaction by occupying reactive sites, or by simply providing resistance to the supply of oxidant or the transport of reaction products. Once the surface is filled with surfactant molecules the additional molecules form multiple layer structures, the added surfactant molecules no longer have direct access to the surface. Consequently, the additional molecules that adsorb at concentrations above the CMC must inhibit corrosion by offering additional resistance to the transport of necessary elements rather than by occupying reactive sites directly.

The corrosion inhibition efficiency decreases with increase in temperature as shown in table-2. Generally, the decrease in the inhibition efficiency with increase in temperature may be explained by the fact that the time lag between the process of adsorption and desorption of inhibitor molecules. Hence, the metal surface remains exposed to the acid environment for a longer period thereby increasing the rate of corrosion with increase in temperature and therefore % IE falls at higher temperatures[7].

Electrochemical impedance spectroscopy measurement: The corrosion behavior of mild steel in 0.5M H_2SO_4 solution in the presence of TDAB was investigated using EIS. Experiments were performed in duplicate and average data is tabulated in table-3. figure-4 a and b shows the Nyquist plots for Mild steel in 0.5M H_2SO_4 and 0.5M H_2SO_4 containing Different concentration (10^{-3}M to 10^{-2}M) of TDAB. The impedance data are analyzed using the circuit shown in figure-5.

Table-3
Impedance parameters for mild steel in 0.5M H_2SO_4 in absence and presence of different Concentration of TDAB at 25°C

Concentration (M)	Y_a (Ω^{-1} cm^{-2} S^{ndl} 10^{-4})	n_a	R_a (Ω)	C_a ($\mu F/cm^2$)	Y_{dl} (Ω^{-1} cm^{-2} S^{ndl} 10^{-4})	n_{dl}	R_{ct} (Ω)	C_{dl} ($\mu F/cm^2$)	IE (%)
Blank	-	-	-	-	15.39	0.8657	5.016	723.6	-
1×10^{-3}	0.8685	1	2.756	86.86	6.658	0.7324	69.66	216.8	92.8
2×10^{-3}	0.9809	1	3.089	98.1	6.565	0.7167	81.68	206.5	93.8
4×10^{-3}	0.9841	1	3.555	98.4	6.205	0.7249	84.13	202.3	94.0
6×10^{-3}	0.911	1	3.643	91.1	6.174	0.7114	95.97	196.2	94.8
1×10^{-2}	0.8942	1	3.936	89.4	5.992	0.7000	117.5	192.2	95.7

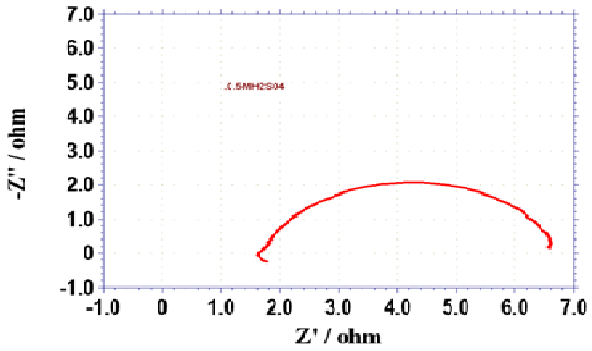

Figure-4a
Nyquist plot for mild steel in 0.5M H_2SO_4

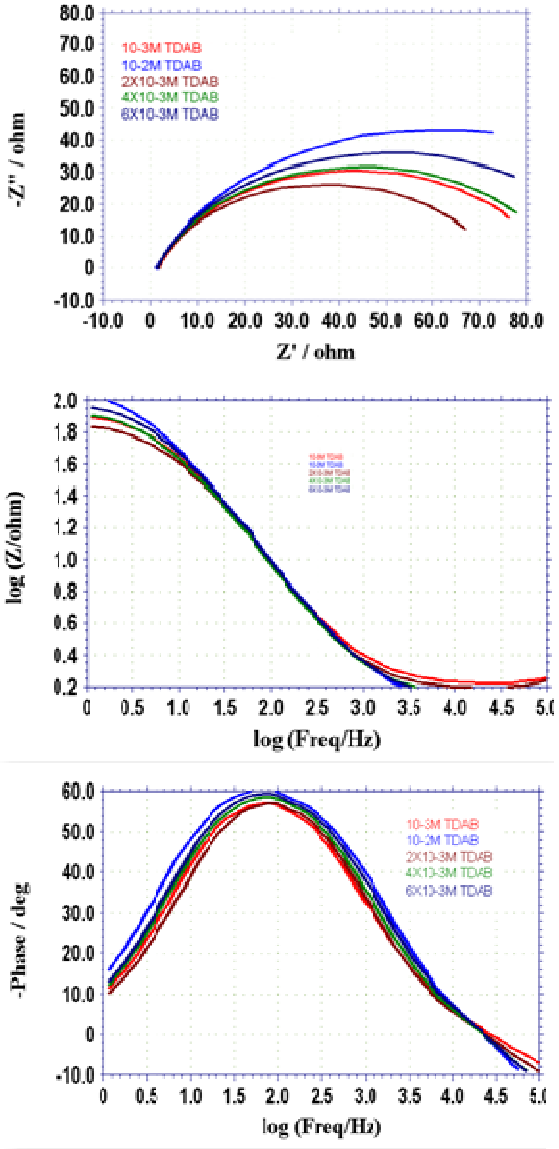

Figure-4b
Nyquist and Bode plots for mild steel in 0.5M H_2SO_4containing different concentrations of TDAB at 25°C

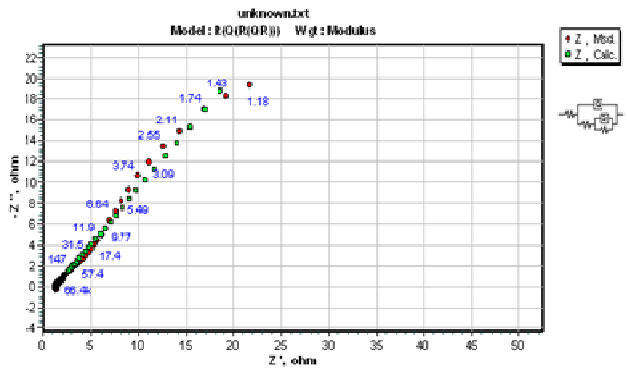

Figure-5
Equivalent circuit model used to fit the impedance data for TDAB in 0.5M H_2SO_4

The fitted data follows almost the same pattern as the experimental results with $R_s(Q_1(R_a(Q_2R_{ct})))$ equivalent circuit using the software Zsimp Win. Where R_s is the solution resistance, Q_1 is the constant phase element (CPE) of the film, R_a is the resistance of the film, Q_2 is the CPE of double layer, and R_{ct} is the resistance of the double layer. The overall response of the system is obtained as a result of the superposition of the responses due to the film (R_a-Q_1) and to the metal-solution interface (R_{ct}-Q_2). It is important to note that the elements (R_a-Q_1) encompass all the information related to the surface layer and the possible defects that may be present within it. On the other hand, all the processes related to charge transfer at the electrical double layer and diffusion transport from the metal-solution interface would be included in the (R_{ct}-Q_2) loop. The impedance parameters for mild steel, without and with TDAB, based on the fitting procedure are tabulated in Table- 3. The following conclusions can be drawn by analyzing the data presented in table-3. It can be seen that the values of n_a is 1 indicates a near capacitive behavior of the surface film formed on the Mild steel sample.

It is observed that the value of C_a associated with Y_a decreases marginally with TDAB addition. As Y_a (C_a) is inversely proportional to thickness of the film, a decrease in C_a implies an increase in the thickness of the film. This increase in thickness may be related to the formation of reaction products as a result of the presence of TDA ions in the solution. It is observed that R_a increases with TDAB addition. C_{dl} corresponding to Y_{dl} decreases with the increase in the TDAB concentration. The decrease in C_{dl} values may be due to the decrease in local dielectric constant and/or increase in the thickness of the double layer. The parameter n_{dl} varied from 0.7 to 0.8 which shows that the diffusion –related processes also play an important role. However, it was observed that the n_{dl} values do not follow any trend. The reason for this could be the lesser number of cathodic intermetallic sites in the mild steel[8]. The R_{ct} values increases as the concentration of TDAB increases. The change in R_{ct} and C_{dl} values were caused by gradual replacement of the

water molecules by the adsorption of the inhibitors on the metal surface. The charge transfer resistance of the Blank increases from 5.016Ω to 117.5Ω upon the addition of 10^{-2}M TDAB which results in 95.7% corrosion inhibition efficiency. This is attributed to the increase in the surface coverage by the inhibitors leading to an increase in inhibition efficiency.

Adsorption isotherm and Thermodynamic parameters: The plot of c/θ against C (Figure-6) for the inhibitor at all temperatures (298K-328K) were straight lines with slopes equal to unity indicating that TDAB obey Langmuir adsorption isotherm given by the equation 5:

$$\frac{C}{\theta} = C + 1/K_{ads} \quad (5)$$

Where C is the concentration of the inhibitor, K_{ads} is the equilibrium constant of the adsorption process and θ is the degree of coverage by the inhibitor molecules on the metal surface, calculated by the relation 6:

$$\theta = \frac{\%IE}{100} \quad (6)$$

Adsorption equilibrium constant K_{ads} is obtained from the intercept of a plot of C/θ as a function of C. and free energy of adsorption were calculated using the relation 7:

$$\Delta G_{ads} = -2.303RT\log(55.5K_{ads}) \quad (7)$$

ΔH^0_{ads} and ΔS^0_{ads} are calculated from the relations 8 and 9:

$$\log\left(\frac{\Theta}{1-\Theta}\right) = \log A + \log C_{Inh} - \frac{Q_{ads}}{2.303RT} \quad (8)$$

Where A is a constant, and Q_{ads} is the heat of adsorption equal to enthalpy of adsorption

Enthalpy of adsorption is obtained from the slope of a plot of $\log\left(\frac{\Theta}{1-\Theta}\right)$ vs 1/T (figure-7) at various concentrations. Entropy of adsorption is calculated from Gibb's Helmholtz equation 9:

$$\Delta G^0_{ads} = \Delta H^0_{ads} - T\Delta S^0_{ads} \quad (9)$$

Where ΔH^o_{ads} is the enthalpy of adsorption, ΔS^o_{ads} is entropy of adsorption, T, Temperature in Kelvin and ΔG^o_{ads} is the free energy of adsorption.

The thermodynamic parameters are tabulated in the table-4. The average value of ΔG^o_{ads} was found to be -30kJ/mol since the values of ΔG^o_{ads} lies between -20kJ/mol and -40kJ/mol indicate that the adsorption mechanism involves two types of interaction, Physisorption and chemisorptions. ΔH^o_{ads} is negative in 0.5M H_2SO_4 which indicates the adsorption of inhibitor molecules on mild steel surface an exothermic process. The negative sign of ΔS^o_{ads} for TDAB in 0.5M H_2SO_4 means decrease in disordering on going from reactants to the metal adsorbed species.

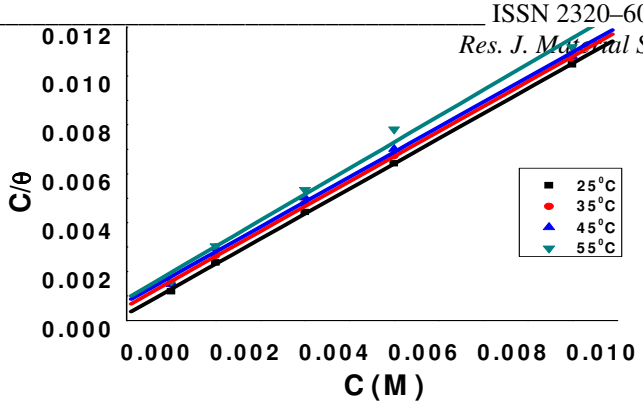

Figure-6
Plot of Langmuir Adsorption isotherm

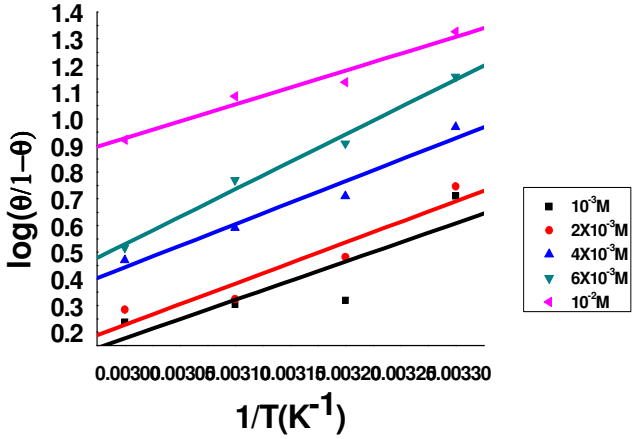

Figure-7
Plot of $\log\left(\frac{\Theta}{1-\Theta}\right)$ vs 1/T

Activation parameters: Arrhenius suggested the famous equation which evaluates the temperature dependence of the corrosion current density as follows 10:

$$\ln i_{corr} = \ln A - \frac{E_a}{RT} \quad (10)$$

Where i_{corr} is the corrosion current density, A is the Arrhenius constant, E_a is the activation energy and R is the universal gas constant. Equation 10 predicts that a plot of lni_{corr} vs 1/T should be a straight line. The slope of the line is $(-\frac{E_a}{R})$ and the intercept of the line extrapolated gives lnA. On the other hand, the change of enthalpy $(\Delta H^{\#})$ and entropy of activation $(\Delta S^{\#})$ for the formation of the activation complex in the transition state can be obtained from the transition state equation11:

$$i_{corr} = \frac{RT}{Nh}\exp\left(\frac{\Delta S^{\#}}{R}\right)\exp\left(\frac{-\Delta H^{\#}}{RT}\right) \quad (11)$$

Where N is Avogadro's constant, h is planck's constant, $\Delta S^{\neq}$ is the change in entropy of activation and $\Delta H^{\neq}$ is the change in enthalpy of activation.

$\Delta S^{\neq}$is obtained from the intercept $\log\left[\left(\frac{R}{Nh}\right)+\left(\frac{\Delta S^{\neq}}{2.303R}\right)\right]$of a plot of $\log\left(\frac{i_{corr}}{T}\right)$ vs 1/T and $\Delta H^{\neq}$ is obtained from the slope $\left(-\frac{\Delta H^{\neq}}{2.303RT}\right)$ of a plot of $\log\left(\frac{i_{corr}}{T}\right)$ vs 1/T.

By using the experimental corrosion current density values obtained from Potentiodynamic polarization measurements for mild steel in 0.5M H_2SO_4 in absence and presence of different concentration of TDAB, plots in accordance with equation (10) and (11) are obtained and illustrated in Figure -8 and 9. All the corrosion kinetic parameters are calculated and tabulated in the Table- 5. It is clear that E_a and $\Delta H^{\#}$ varied in the same fashion. As observed, E_a and $\Delta H^{\#}$ for the inhibited solutions were higher than that for the uninhibited solutions. This could be attributed to the presence of an energy barrier for the corrosion reaction due to the existence of inhibitor cations at the metal /electrolyte interface.

Table-4
Thermodynamic parameters obtained from adsorption isotherms for TDAB in 0.5M H_2SO_4

0.5M H_2SO_4						
TDAB						
Temperature (K)	**R**	**Slope**	**K_{ads}**	**ΔG^{o}_{ads} (kJ/mol)**	**ΔH^{o}_{ads} (kJ/mol)**	**ΔS^{o}_{ads} (J/mol/K)**
298	0.9998	1.0248	3882.9	-30.4	-30.3	0.3
308	0.9997	1.0208	1717.5	-29.3	-30.3	-3.2
318	0.9983	1.0197	1299.9	-29.6	-30.3	-2.2
328	0.9950	1.0644	1106.8	-30.1	-30.3	-0.6

Table-5
Corrosion kinetic parameters for mild steel in 0.5M H_2SO_4 in absence and presence of different concentrations of TDAB

Concentration (M)	**E_a (kJ/mol)**	**$\Delta H^{\neq}$ (kJ/mol)**	**$\Delta S^{\neq}$ (J/mol/K)**
Blank	42.6	39.9	-155.3
1×10^{-3}	63.0	53.3	-123.2
2×10^{-3}	65.0	54.5	-120.1
4×10^{-3}	65.2	54.3	-96.0
6×10^{-3}	69.6	58.4	-110.9
1×10^{-2}	76.6	64.0	-131.4

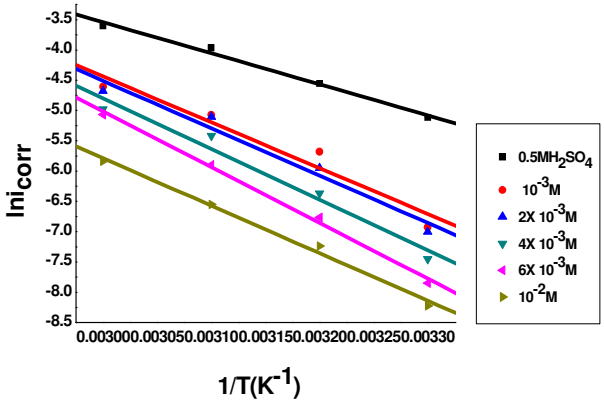

Figure-8
Arrhenius plots for MS in 0.5M H_2SO_4 without and with various concentration of TDAB

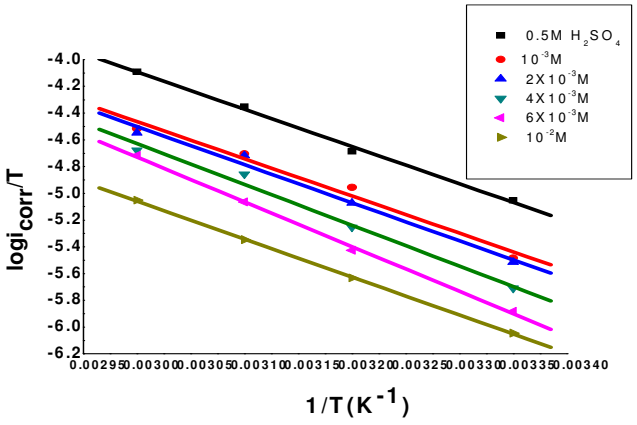

Figure-9
Transition plots for MS in 0.5M H_2SO_4 Without and with various concentration of TDAB

The values of E_a were higher for the inhibited solutions than that for the uninhibited solution (42.6 kJ/mol), which may be interpreted as physical adsorption that occurs in the first stage. But Behpour et al[9] have explained the change in the activation energy from energetic heterogeneity of the surface. If energetic surface heterogeneity is assumed, active centers of surface have different energy. There are two possibilities: in the first case the inhibitor is adsorbed on the most active adsorption sites (having the lowest energy) and the corrosion process takes place predominantly on the active sites of higher energy (resulting in higher activation energy). In the second case a smaller number of more active sites remain uncovered which take part in the corrosion process (resulting in the lower activation energy).

Vracar and Drazic[10] have argued that the adsorption type obtained from the change of activation energy, cannot be taken as decisive due to competitive adsorption with water whose removal from the surface also requires some activation energy. On the other word, physisorption process may contain chemisorption simultaneously and vice versa. The increase in activation energy can be attributed to an appreciable decrease in the adsorption of the inhibitor on the steel surface with the increase in temperature[11]. The values of E_a increases with an increase in inhibitor concentration, suggesting strong adsorption of inhibitor molecules at the metal surface. The increase in the activation energy is due to the corrosion reaction in which charge transfer was blocked by the adsorption of TDAB molecules on the mild steel surface. It is also revealed that the whole process was controlled by the surface reaction since the energy of activation in both the absence and presence of TDAB was greater than 20kJ/mol.The entropy of activation ($\Delta S^{\#}$) in the blank and inhibited solutions is large and negative indicating that the activated complex represents association rather than dissociation step. This implies that a decrease in disorder occurred when proceeding from the reactants to the activated complex. In addition, the less negative values of $\Delta S^{\#}$ in the presence of inhibitor imply that the presence of inhibitor created a near equilibrium corrosion system state.

Scanning electron microscopic studies: Figure-10a shows the surface morphology of the polished mild steel surface before immersion in 0.5M H_2SO4. SEM photographs after specimen immersion in 0.5M H_2SO_4 for 3h in the absence and presence of an optimum concentration of TDAB are shown in the figure-10b and10c respectively. It could be seen from the figure-10 b that the specimen surface is strongly damaged and faceting seen in the figure as a result of pits formed due to the exposure of mild steel to the acid in the absence of the inhibitor. From the Figure- 10c it could be seen that in the presence of inhibitors, the faceting disappears and the surface was free from pits and it was smooth. This reveals that there is a good protective film adsorbed on specimen surface, which was responsible for inhibition of corrosion.

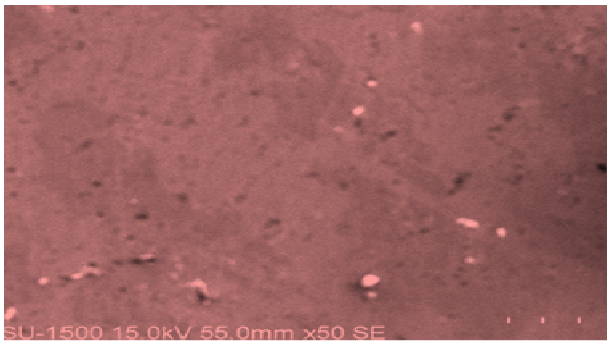

(a)

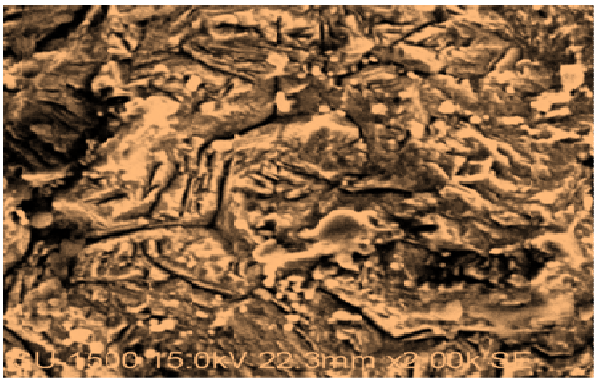

(b)

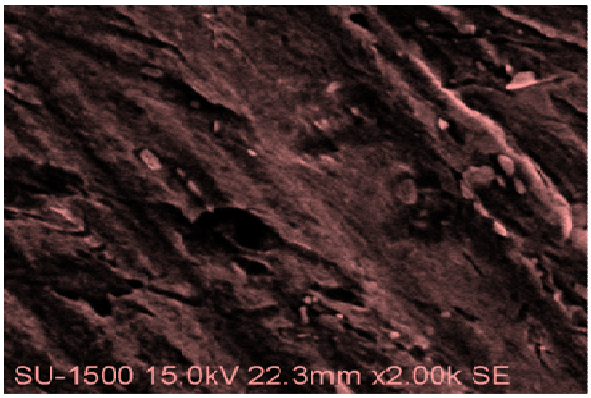

(c)

Figure-10
Surface Characterization by SEM for a) Polished mild steel b) in 0.5M H_2SO_4 in c) in TDAB

Mechanism: Fe electro-dissolution in acidic sulphate solutions depends primarily on the adsorbed intermediate [FeOH]ads as follows[12]:

$$Fe + H_2O \longrightarrow [FeOH]ads + H^+ + e^-$$

$$[FeOH]ads \longrightarrow [FeOH]^+ + e^- \text{ (Rate determining step)}$$

$$[FeOH]^+ + H^+ \longrightarrow Fe^{2+} + H_2O$$

The cathodic hydrogen evolution follows the steps:

$$Fe + H^+ \longrightarrow [Fe\,H^+]ads$$

$$[Fe\,H^+]ads + e^- \longrightarrow [FeH]ads$$

$$[FeH]ads + H^+ + e^- \longrightarrow Fe + H_2$$

The corrosion rate of iron in H_2SO_4 solutions is controlled by the hydrogen evolution reaction and dissolution reaction of iron. In the presence of halide ions(X^{-1}), the mechanism for the anodic dissolution is given as

$$Fe + H_2O + X^- \longrightarrow [FeXOH]^-_{ads} + H^+ + e^-$$
$$[FeXOH]^-_{ads} \longrightarrow [FeXOH] + e^- \text{ (rate determining step)}$$
$$FeXOH + H^+ \longrightarrow Fe^{2+} + X^- + H_2O$$

The process of adsorption is influenced by the nature and charge of the metal, chemical structure of inhibitor and the type of aggressive electrolyte. The charge of the metal surface can be determined from the potential of zero charge (PZC) on the correlative scale (Øc) by the equation

$$Ø_c = E_{corr} - E_{q=0}SS$$

Where Eq=0 is the potential of the zero charge. However, a value obtained in H_2SO_4 is -502.8 mV vs SCE. The PZC of iron is -550mV in H_2SO_4, therefore Øc is positive (+47.2) and hence the mild steel surface acquires positive charge. In strong acid solution, studied inhibitors, ionizes and carry a positive charge. As Steel surface is positively charged in presence of H_2S0_4 medium, while Bromide ion is negatively charged, as a result the specific adsorption of bromide ion occurs onto mild steel surface, causing negatively charged surface of steel. By means of electrostatic attraction, surfactant cation easily reaches mild steel surface, so bromide ion acts as an adsorption mediator for bonding metal surface and inhibitor. This gives rise to the formation of an adsorption composite film in which Br^{-1} ion are sandwiched between metal and positively charged part of inhibitor. This film acts as a barrier facing corrosion process.

Conclusion

i. Corrosion inhibition efficiency increases with Concentration but decreases with increase in temperature. ii. EIS measurement showed that the charge transfer controls the corrosion process. iii. Investigated surfactant inhibits the corrosion of mild steel in 0.5M H_2SO_4. iv. Polarization data shows that the investigated surfactant acts as mixed type inhibitor. v. Results obtained from the weight loss, Tafel polarization and EIS are in good agreement.

Acknowledgement

The Authors Thank SINSIL International, Bangalore (Roopsingh Y.R, GM) for providing their Instrument Model CHI660C, Electrochemical Work station (CH Instruments Inc., USA)

References

1. Dourna Asefi., Mokhtar Arami., Niyaz Mohammad sMahmoodi., Electrochemical effect of cationic gemini surfactant and halide salts on corrosion inhibition of low carbon steel in acidic medium, ECS Transaction., **33(30),** 1-16 **(2011)**

2. Atia A.A. and M.M. Saleh., Inhibition of acid corrosion of steel using cetylpyridinium chloride, *J. Appl. Electrochem*., **33**, 171**, (2013)**

3. Dourna Asefi., Ali asghar Sarabi and Mokhtar Arami., Corrosion Inhibition Effect of Cationic Surfactant and Synergistic Effect of the Presence of the Chloride Ions, ECS transaction, **19**, 135-140 **(2009)**

4. Fouda A.S., H.K. AbdEl-Aziz and Y.A. Elewady., Corrosion inhibition of carbon steel by cationic surfactants in 0.5M HCl solution, *Journal of chemical science and Technology*, **1(2),** 45-53**(2012)**

5. Kumar Harish and Sunita., ADS, ALS, AHDS and ADDBS Surfactants as Corrosion Inhibitors for Carbon Steel in acidic Solution, *Research journal of chemical sciences*, **2(7),** 1-6 **(2012)**

6. Free M.L., Understanding the effect of surfactant aggregation on corrosion inhibition of mild steel in acidic medium*, Corros. Sci.,* **44,** 2865 **(2002)**

7. Kalpana Bhrara., Gurmeet Singh and Hansung Kim., *Inhibiting effects of Butyl triphenyl phosphonium bromide on corrosion of mild steel in 0.5M sulphuric acid solution and its adsorption characteristics, Corrosion Sci.,* **50**, 2747-2754 **(2008)**

8. Mishra A.K. and R. Balasubramaniam., Corrosion inhibition of Aluminium Alloy 6061 by Rare Earth Chloride, Corrosion., **63(3),** 240-248 **(2007)**

9. Behpour M., S.M. Ghoreishi, N. Soltani and M. Salavati-Niasari., The inhibition effect of some bis- n-bidentate schiff bases on corrosion behavior of 304 stainless steel in hydrochloric acid solution, *Corros.Sci.,* **51**, 1073 **(2009)**

10. Szauer T. and A. Brandt., On the role of fatty acid in adsorption and corrosion inhibition of iron by amine-fatty acid salts in acidic solution, *Electrochim. Acta.,* **26,** 1257-1260 **(1981)**

11. Solmaza R., G. Kardaş., M. Çulha., B. Yazici, and M. Ebril., Investigation of adsorption and inhibitive effect of 2-mercaptothiazoline on corrosion of mild steel in hydrochloric acid media, *Electrochim. Acta,* **53**, 5941-5952 **(2008)**

12. Prathibha B.S., P. Kotteeswaran and V. Bheemaraju., Study on the inhibition of mild steel corrosion by quaternary ammonium compounds in sulphuric acid medium, *Res. J. Rescent Sci*., **2(4),** 1-10**(2013)**